Accepted Manuscript

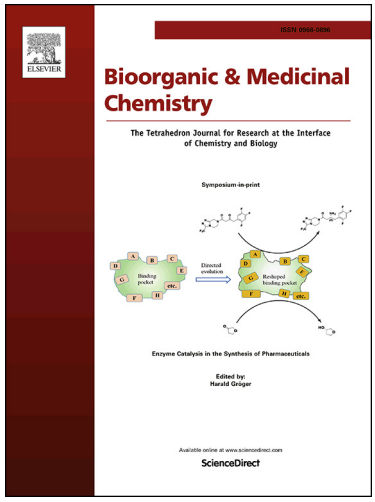

Design, synthesis and algicides activities of thiourea derivatives as the Novel Scaffold Aldolase Inhibitors

Shan Xiao, Lin Wei, Zongqin Hong, Li Rao, Yanliang Ren, Jian Wan, Lingling Feng

PII: S0968-0896(18)31044-7
DOI: https://doi.org/10.1016/j.bmc.2019.01.023
Reference: BMC 14715

To appear in: *Bioorganic & Medicinal Chemistry*

Received Date: 8 November 2018
Revised Date: 17 January 2019
Accepted Date: 22 January 2019

Please cite this article as: Xiao, S., Wei, L., Hong, Z., Rao, L., Ren, Y., Wan, J., Feng, L., Design, synthesis and algicides activities of thiourea derivatives as the Novel Scaffold Aldolase Inhibitors, *Bioorganic & Medicinal Chemistry* (2019), doi: https://doi.org/10.1016/j.bmc.2019.01.023

Bioorganic & Medicinal Chemistry
journal homepage: www.elsevier.com

Design, synthesis and algicides activities of thiourea derivatives as the Novel Scaffold Aldolase Inhibitors

Shan Xiao,‡ Lin Wei,‡ Zongqin Hong, Li Rao, Yanliang Ren* and Jian Wan* and Lingling Feng

International Cooperation Base of Pesticide and Green Synthesis (Hubei), Key Laboratory of Pesticide & Chemical Biology (CCNU), Ministry of Education, Department of Chemistry, Central China Normal University, Wuhan 430079, China

ARTICLE INFO

Article history:
Received
Received in revised form
Accepted
Available online

Keywords:
Aldolases
Fragment-based Virtual Screen
thiourea
algicides activities
De novo Discovery

ABSTRACT

By using a new Fragment-Based Virtual Screen strategy, two series of novel FBA-II inhibitors (thiourea derivatives) were *de novo* discovered based on the active site of fructose-1, 6-bisphosphate aldolase from Cyanobacterial (CyFBA). In comparison, most of the *N*-(2-benzoylhydrazine-1-carbonothioyl) benzamide derivatives (**L14~L22**) exhibit higher CyFBA-II inhibitory activities compared to *N*-(phenylcarbamothioyl) benzamide derivatives (**L1~L13**). Especially, compound **L14** not only shows higher CyFBA-II activity (K_i = 0.65 μM), but also exhibits most potent *in vivo* activity against Synechocystis sp. PCC 6803 (EC_{50}=0.09 ppm), higher (7-fold) than that of our previous inhibitor (EC_{50}=0.6 ppm). The binding modes of compound **L14** and CyFBA-II were further elucidated by jointly using DOX computational protocol, MM-PBSA and site-directed mutagenesis assays. The positive results suggest that strategy adopted in this study was promising to rapidly discovery the potent inhibitors with novel scaffolds. The satisfactory algicide activities suggest that the thiourea derivatives is very likely to be a promising lead for the development of novel specific algicides to solve Cyanobacterial harmful algal blooms (CHABs).

* Corresponding author. Tel.: +86-027-67862022; fax: +86-027-67862022; e-mail: renyl@mail.ccnu.edu.cn;jianwan@mail.ccnu.edu.cn

‡ These authors contributed equally to this study

1. Introduction

Cyanobacterial harmful algal blooms (CHABs) have been increasing in frequency all over the world.[1] Toxin-producing CHABs have directly threatened to the human health, living resources, and water economies.[2-5] To control these CHABs, many approaches included mechanical, physical/chemical, and biological controls have been used so far.[6] In comparison, chemical control was the most effective method. Chemical control involves the use of compounds (copper compounds, chemical oxidants, and herbicides).[1, 7] Especially, the compounds designed for the specific target of cyanobacteria provide us a useful pathway to the development of potential algaecides. Previously, using the systematically structure-centric approach, several novel inhibitors of class II fructose-1, 6-bisphosphate aldolase from Cyanobacteria (CyFBA-II) were designed and synthesized in our group.[8, 9] In contrast, the N-(2,5-Dioxo-2,5-dihydro-1H-pyrrol-1-yl) benzamide derivatives exhibit higher inhibitory activities against Synechocystis sp. PCC 6803.[9] However, the instability of those compounds limits their further applications. To address this concern, two series of novel scaffold CyFBA-II inhibitors (thiourea derivatives) were *de novo* designed by using Fragment-Based Virtual Screen (FBVS) strategy developed in our group based on the substrate site of CyFBA-II. The proposed binding model of novel inhibitors targeting into CyFBA-II were systematically identified by integrating Docking-ONIOM-XO (DOX)[10] computational protocol, Molecular Mechanics combined with the Poisson–Boltzmann and Surface Area continuum solvation (MM-PBSA),[11] chemical synthesis, and site-directed mutant assays.

2. Results and Discussion

2.1. Design of thioureas derivatives as novel CyFBA-II inhibitors

In previous work, we found that *N*-(2,5-Dioxo-2,5-dihydro-1*H*-pyrrol-1-yl) benzamide derivatives shown potent inhibition against CyFBA-II.[8] However, these compounds appears to be unstable due to the hydrazone moiety. Recently, *de novo* design (i.e. FBVS) are well-developed and mature technique for lead discovery as well as lead optimization.[12, 13] Some *de novo* design computational methods have already been implemented in commercial or academic software, such as LUDI,[14] EA-inventor,[15] SPROUT,[16] BUILDER,[17] PROLIGANDS,[18] LigBuilder[19] and LEA3D,[20] especially, many protocols have successfully applied to the discovery of highly potent inhibitors.[21-23] However, most of the software mentioned-above were performed based on their specific docking algorithm and scoring function. Our previous studies[8, 9, 24] suggested that Surflex-Dock,[25] evaluated by using an empirical function ChemScore, was suitable for the discovery of novel FBA inhibitors, thus Surflex-Dock were used in the present FBVS protocol to generate and score the conformations of fragments and resulting compounds based on the CyFBA-II active pocket. To design the algaecides with desirable druglike properties, several rings and frameworks in FDA-approved drugs[26] were used as the fragments dataset (**Figure S1**) for this FBVS protocol (**Figure 1**).

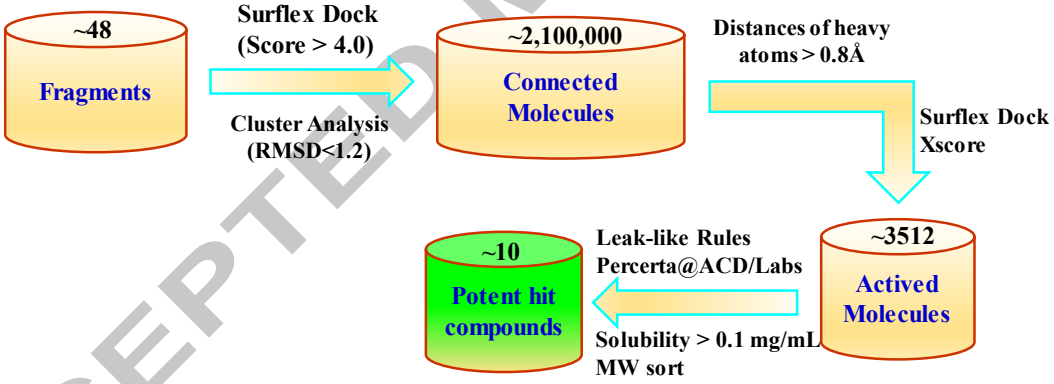

Figure 1. Fragment-Based Virtual Screen (FBVS) protocol

The 3D-Conformation of CyFBA-II were constructed as our previous work.[8, 9] The Zinc ion (Zn^{2+}) were derived from the template structure (PDB ID: 3GAY). The Molecular Dynamics (MD) simulation of CyFBA-II and substrate (FBP) were performed prior to the docking, as illustrated in **Figure S2** and **Figure S3** in supporting information. In MD procedure, the charge of Zn ion is set as 2, the parameters of Zn ion is optimized by Pang group[27, 28] in Amber package. For the FBVS protocol, the fragments were docked firstly into the active pocket of CyFBA-II by using Surflex-Dock. Twenty poses were generated for each fragment. Then, the cluster analysis for each fragment were performed (RMSD < 1Å), and six conformations with high score (surflex-dock score/number of atoms > 0.15) will be selected for the connection between fragments. Subsequently, about 3512 molecules were generated by using the connection module developed by our group. After that, the building compounds will be docked again into the CyFBA-II using Surflex-Dock, and the Xscore developed by Wang et al.,[29] were performed for all docking conformations. Then, top 500 compounds with high average score (Ave_score) of protein-ligand given by X-score were selected for the further Lead-like evaluation by using Percepta@ACDLabs software. At this step, about 174 reasonable compounds were remained. Finally, top 10 compounds with smaller Molecular Weight (MW) and solubility larger than 0.1 mg/mL were selected for our further analysis. Top 10 potent hit compounds generated by FBVS routing were listed in **Table 1**.

Table 1. The top 10 hit compounds generated by present FMVS protocol

*ID	Compounds	LogP[a]	H-Bonds[b]	Solubility[a]	Avg score[c]
372	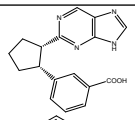	2.96	8	13.13	6.12
299	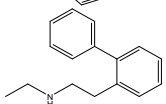	4.00	2	8.35	6.21
453	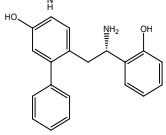	3.23	6	6.35	6.16
247	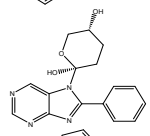	0.94	9	0.73	6.09
157	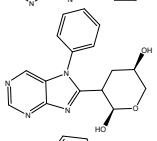	0.82	9	0.44	6.18
406	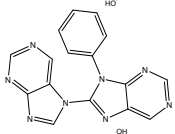	0.99	8	0.29	6.09
278	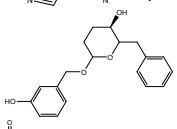	3.32	6	0.20	6.35
435 (L1)	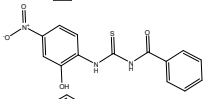	2.60	10	0.18	6.13
154	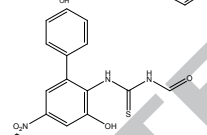	2.48	10	0.16	6.19
245	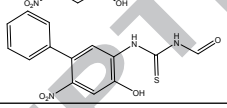	2.45	10	0.16	6.22

According to the total number of HDonors&HAcceptors and synthesis step number, compound **435**, which was re-named **L1**, was finally selected to further investigation; The synthetic route were illustrated in **Scheme 1**, which has been documented by Rauf et al.[30]

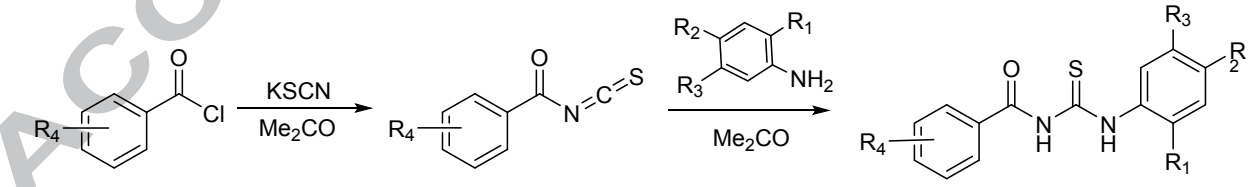

R_1 = H, OH, Cl, NO_2; R_2=H, NO_2, Br; R_3=H, NO_2; R_4=H, CF_3, CH_3, Ph, NO_2, Cl

Scheme 1. General synthetic route for compound **L1~L13.**

Fortunately, the inhibitory constant (K_i) of **L1** against CyFBA-II was of 16.7 μM (**Table 2**), this result indicates the FBVS route adopted in the present study seems to be reliable.

2.2. Structure-activity-relationship (SAR) analysis

To discover more potent CyFBA-II inhibitors, it is necessary to analyze the structure-activity-relationship (SAR). Firstly, we fixed R_2, R_3 and R_4 to Hydrogen, and introduced the Cl, NO_2, and OH group into R_1 position (Table 2). However, no remarkable CyFBA-II inhibition (Inhibition Rate < 40%) were observed, such as compounds **L2 ~ L4**. In comparison, compound **L4** exhibit higher inhibition rate (37%) than those of **L2** and **L3**. This indicate that hydroxyl group seems to be favorable in R_1 position. Furthermore, R_1, R_3 and R_4 were fixed to hydrogen, and R_2 was replaced by OH (**L5**), Br (**L6**) and NO_2 (**L7**), the results show that compound **L7** have relatively high inhibition rate (60%) compared with those of compounds **L5** (22%) and **L6** (42%). Taken together, we believe that OH at R_1 and

NO_2 at R_2 position appears to be favorable. To explain this experiment observation, **L11** was chosen as the representative compound, the binding model of **L11** and CyFBA-II was predicted by using the DOX strategy, which has been documented previously.[10] The possible binding conformation of **L11** and CyFBA-II was illustrated in **Figure 2**.

Table 2. Substitution patterns of compounds **L1 – L13** and their inhibition activity against CyFBA-II

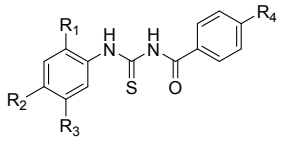

Compds	R_1	R_2	R_3	R_4	K_i (μM)/ Inhibition Rate[a]
L1	OH	NO_2	H	H	16.7±0.4
L2	Cl	H	H	H	30%[a]
L3	NO_2	H	H	H	15%[a]
L4	OH	H	H	H	37%[a]
L5	H	OH	H	H	22%[a]
L6	H	Br	H	H	42%[a]
L7	H	NO_2	H	H	60%[a]
L8	OH	NO_2	H	CF_3	5.5±0.10
L9	OH	NO_2	H	CH_3	5.5±0.20
L10	OH	NO_2	H	Ph	2.5±0.10
L11	OH	NO_2	H	NO_2	1.9±0.02
L12	OH	H	NO_2	H	9.1±0.20
L13	OH	H	NO_2	Cl	9.1±0.10

As shown in **Figure 2**, the hydroxyl group and sulfur of **L11** can coordinate with the Zn^{2+}. Moreover, the hydroxyl can also form hydrogen bond with residue N275. To verify the importance of residue N275, the site-directed mutagenesis was performed. As listed in **Table 3**, the inhibitory activity of **L11** against N275A (37.9μM) decreased about 20-fold than parental CyFBA-II (1.9 μM), the possible reason for this case is that N275A results in the disappear of the hydrogen-bond between N275 and the hydroxyl moiety in benzene ring (Figure 2). Additionally, Figure 2 illustrate that the nitro group in R_2 position can form hydrogen bonds with residues K202 and T278. As expected, the inhibitions of **L11** against T278A decreased about 46.3-fold than parental CyFBA-II (**Table 3**). Unfortunately, K202A mutant lacked detectable enzymatically activity, thus the interaction of compound and K202 could not be determined using mutagenesis experiment. Combing the DOX results (**Figure 2**), we believe that the interaction between nitro group in R_2 position and T278 is probably existed. Therefore, the compounds with hydroxyl group in R_1 and NO_2 group in R_2 position could exhibit high inhibitory activities against CyFBA-II.

Subsequently, we fixed R_1 and R_2 to OH and NO_2, and tried to vary the R_4 to CF_3 (**L8**), CH_3 (**L9**), Ph (**L10**) and NO_2 (**L11**). Compared with **L1** (16.7 μM), **L8 ~ L11** show higher inhibitions (K_i =1.9~5.5 μM) against CyFBA-II. Especially, the **L11** exhibit highest CyFBA-II inhibitions with K_i value of 1.9 μM. These findings reveal that the introduction of substituents in R_4 position, hydrophilic or hydrophobic group, might improve the CyFBA-II inhibitions of hit compounds. However, our DOX prediction (**Figure 2**) show that the nitro group in R_4 position locate outside of the active pocket, no remarkable interactions of nitro group in R_4 position could be observed. Therefore, the reason that compounds L8~L11 have higher CyFBA-II inhibitions is not clear so far.

In addition, one can notice from **Table 2** that **L12** exhibit higher inhibitory activity (9.1 μM) compared with compound **L4** (37%), this indicate that the NO_2 in R_3 position seems to be favorable than H. The reason is likely that NO_2 in R_3 position could also form hydrogen-bond with T278.

One can notice from **Figure 2** that, the NH moiety in the middle linkage of **L11** might form a hydrogen-bond with D277, and the carboxyl group of **L11** may form hydrogen-bond with residues R281 and R302. However, the D277A mutant couldn't affect the inhibitory activity of **L11** (2.4-fold), this is not consistent with the predicted interaction in **Figure 2**, maybe due to the flexibility of residue D277. In contrast, the mutants of R281A and R302A could result in 12.9 and 76-fold decrease of the **L11** inhibitions (**Table 3**). In addition, the Van der Waals interaction between thiourea linkage and R281 could also be observed in **Figure 2**. These may be the partial reason that the inhibitions of **L11** against R281A significantly decreased about 76-fold compared with parental CyFBA-II.

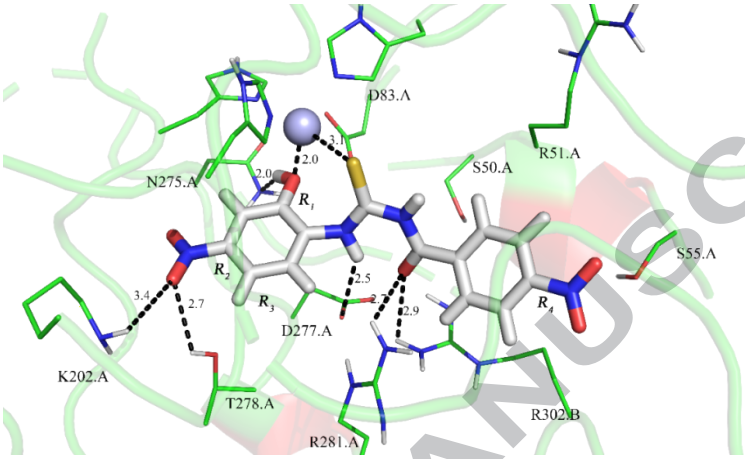

Figure 2. The predicted binding modes of compound **L11** and CyFBA-II

2.3. Optimization of hit compounds.

Based upon the mutant data (**Table 3**), it is concluded that R281 is significantly important for the binding of **L11** against CyFBA-II. However, due to the effect of the coordination between sulfur and Zn^{2+}, the hydrogen-bond distance of **L11** and R281 is larger than 3 Å (**Figure 2**). Thus, we propose that if one amide group were interposed between hydroxyl and sulfur, the hit compounds will be closer to R281, which in turn improve the inhibitory activities of hit compounds against CyFBA-II. For this purpose, **L14~L22** were further synthesized (**Table 4**), the synthetic route was illustrated in **Scheme 2**.

Table 3. The K_i values of the compound **L11** and **L14** against wildtype (WT) and mutants of CyFBA-II

	L11(μM)		**L14** (μM)	
	K_i	K_i(mutant)/K_i(WT)	K_i	K_i(mutant)/K_i(WT)
WT	1.9±0.02	1	0.7±0.02	1
S50A	3.9±0.20	2.1	15.2±0.30	23.4
R51A	3.3±0.20	1.7	3.9±0.50	6.0
S55A	3.4±0.10	2.1	1.0±0.10	1.5
N275A	37.9±1.4	20	15.9±1.0	24.5
D277A	4.6±0.60	2.4	7.2±0.50	11
T278A	87.5±0.50	46.3	4.3±0.50	6.6
R281A	143.7±1.5	76.0	52.3±0.40	80.5
R302A	24.4±1.1	12.9	20.4±0.10	31

As listed in **Table 4**, most of these compounds have high inhibitory activities against CyFBA-II (K_i ⩽ 5.2 μM). When R_1 was replaced by hydroxyl group, the compounds (**L14~L16**) exhibit higher inhibitory activities against CyFBA-II (K_i =0.65~0.88μM). Especially, compound **L14** exhibits highest inhibition with K_i of 0.65 μM. These results indicate that the hydroxyl group in R_1 position are significantly important for the inhibitory activities of hit compounds. The possible binding modes (**Figure 3**) of compound **L14** and CyFBA-II were also predicted by using DOX strategy and MD simulation, the plots of MD were illustrated in **Figure S4**.

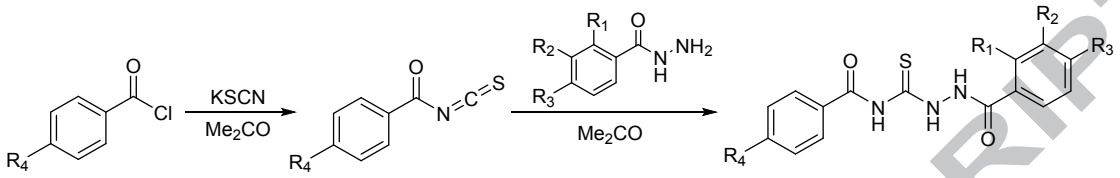

R_1=H, OH; R_2=H, Br, NO_2; R_3=H, OH, F, Br, NO_2; R_4=H, F, Cl

Scheme 2. General synthetic route for **L14~L22**

Similar to **L11**, the hydroxyl group in R_1 of **L14** could form hydrogen bond with N275 (**Figure 3**). When N275 was mutated to Ala, the inhibitions of **L14** against N275A decreased about 25-fold compared to WT. Therefore, we believe that the hydrogen-bond between N275 and **L14** is essential for binding of **L14** and CyFBA-II (**Figure 3**).

Table 4. Substitution patterns of compounds **L14 – L22** and their inhibition activity against CyFBA-II and Synechocystis sp. PCC 6803

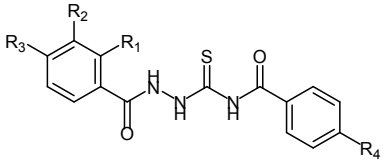

Compds	R_1	R_2	R_3	R_4	K_i (μM)	EC_{50} (ppm)
L14	OH	H	H	H	0.65±0.05	0.09±0.02
L15	OH	H	H	Cl	0.63±0.03	0.98±0.34
L16	OH	H	H	F	0.88±0.03	5.36±0.73
L17	OH	H	OH	H	1.25±0.16	6.4±0.80
L18	H	NO_2	H	H	1.87±0.09	0.39±0.13
L19	H	Br	H	H	3.1±0.17	5.9±1.1
L20	H	H	F	H	3.5±0.71	8.2±0.60
L21	H	H	Br	H	5.2±0.10	1.58±0.20
L22	H	H	NO_2	H	2.8±0.12	16.3±6.2

Additionally, one carbonyl group in the left of the thiourea linkage could coordinate with Zn^{2+}, while the other carbonyl group could form coordination with Zn^{2+} via water molecule (**Figure 3**). The remarkable hydrogen bonds between thiourea linkage and surrounding residues (S50, R281 and R302) could be

observed. As expected, when the S50, R281 and R302 were mutated to Ala, the corresponding inhibitory activities of **L14** decrease about 23.4, 80.5, 31-fold (**Table 3**). This is satisfactory consistent with our theoretical predictions that these three residues could form hydrogen bond with compound **L14**. Noticeably, the R281A mutant could result in the 80-fold decrease of **L14** inhibitory activities (Figure 3), this is owning to the Van der Waals interaction between thiourea linkage and R281 and R302, which is similar to the binding-modes of **L11** and CyFBA-II (**Figure 2**).

It should be noticed that the NO_2 moiety of **L11** can form a hydrogen-bond with T278 (**Figure 2**), the K_i of **L11** against T278A is significantly increased 46.3-fold (**Table 3**) compared to parental CyFBA-II. In contrast, no hydrogen-bond between **L14** and D278 could be formed (**Figure 3**), thus the effect of D278A on the inhibitory activity of **L14** is slightly, with the decrease of 6.6-fold (**Table 3**). In addition, our DOX&MD results show no interaction between **L14** and residues R51 and S55. As expected, when S55, R51 were mutated, the corresponding K_i value decreased less than 10-fold. The well agreement between experimental and theoretical results show that our predicted interactions between **L14** and CyFBA-II is reasonable.

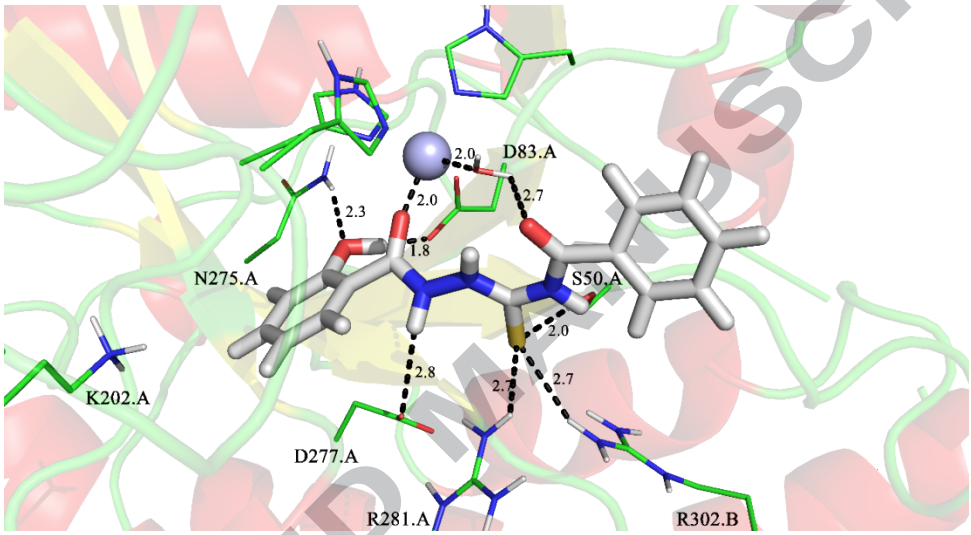

Figure 3. The possible binding modes of **L14** and CyFBA-II obtained by DOX strategy and molecular dynamic (MD) simulations

The R_4 substituent of hit compound located out of the active cavity, therefore, our substituent in R_4 position actually couldn't improve the inhibition activities of hit compounds, such as **L14~L16.**

Furthermore, the binding free energies of **L14** and the mutants (N275A, R281A, S50A and R302A) were also calculated by using MMGBSA method based on the MD results. Our MMGBSA results (**Table 5**) show that the R281A and R302A could result in the remarkable decrease (6.29 and 6.21 kcal/mol) of $\Delta\Delta G_{bind}$, while R275A and S50A mutants could lead to relatively small decrease (5.99 and 3.44 kcal/mol) of $\Delta\Delta G_{bind}$. These are qualitatively agreement with the experimental K_i value. Taken together, we could believe that the binding modes of **L14** and CyFBA-II predicted by DOX and MD were reasonable, and R281 maybe a critical pharmacophore to the binding of hit compounds.

2.4. Synechocystis Activity

The inhibition activities (EC_{50}) of compounds **L14~L22** against Synechocystis sp. PCC 6803 were further determined (**Table 4**). As listed in **Table 4**, most compounds with high CyFBA-II inhibition activities generally exhibit potent Synechocystis activities. For example, the inhibition constant (K_i) of compounds **L14 ~ L22** were less than 6 μM, correspondingly, the EC_{50} of most of these compounds is less than 10 ppm. Especially, compound **L14** shows highest CyFBA-II inhibition activity (0.65μM), and also exhibits most potent algicide activity (EC_{50} = 0.09 ppm) which is 7-fold potent than our previous inhibitor (**Y10**) with EC_{50} of 0.6 ppm.[24] However, it is hard to make direct correlations between CyFBA-II inhibitions and algicide activities from the currently available experimental data, because the absorption, distribution, and metabolism performance of individual compound obtained in the present study. For instance, the CyFBA-II inhibitory activities of compounds **L16** (0.88μM), **L17** (1.25μM) and **L22** (2.7μM) is higher, but these compounds show relatively weak algicide activities, with the EC_{50} of 5.36 ppm, 6.4 ppm, and 16.3 ppm, respectively.

Table 5. Binding free energy of compound **L14** and mutant and wild-type (WT) enzyme of CyFBA-II calculated by MMGBSA, together with experimental K_i values

	ΔGbing(kcal/mol)	ΔΔGbind(kcal/mol)	K_i(μM)	K_i(mutant)/K_i(WT)
WT	-30.56	0	0.65±0.02	1
N275A	-24.57	5.99	15.93±1.0	24.5
R281A	-24.27	6.29	52.34±0.41	80.5
S50A	-27.12	3.44	15.2±0.29	23.4
R302A	-24.35	6.21	20.44±0.14	31.0

To further confirm that the algicide activities of these hit compounds is achieved by inhibiting CyFBA-II enzyme, the inhibition of the representative compound **L14** against overexpressed Synechocystis sp. PCC 6803 (PSBII), whose FBA-II gene was overexpressed (Figure 4B). Due to the increase of FBA-II gene in Synechocystis sp. PCC 6803, the algicide activity of **L14** against PSBII (EC_{50}=4.98μM, Figure 5B) was decreased about 18-fold compared to the activity of **L14** against WT Synechocystis sp. PCC 6803 (EC_{50}=0.28μM). The result demonstrated that **L14** could actually inhibit CyFBA-II in Synechocystis sp. PCC 6803, in turn inhibit the growth of the Cyanobacterial.

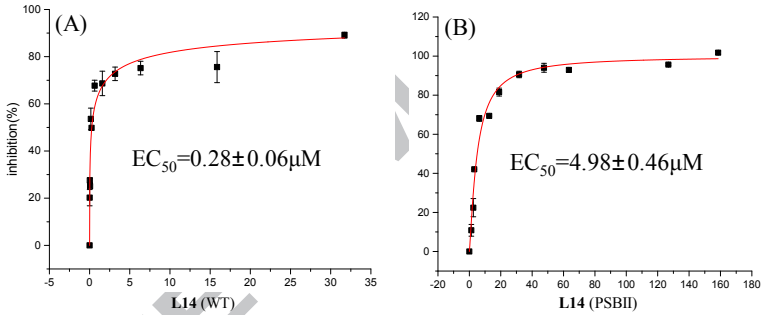

Figure 4. The inhibition curve of compound L14 against Synechocystis sp. PCC 6803. (A) Synechocystis sp. PCC 6803 from wild-type (WT) strains; (B) Synechocystis sp. PCC 6803 from CyFBA-II overexpression strains (PSBII).

3. Conclusions

Herein, using a new Fragment-Based Virtual Screen (FBVS) strategy developed in our group, two series of novel FBA-II inhibitors (thiourea derivatives) were *de novo* discovered based on the active site of fructose-1, 6-bisphosphate aldolase from Cyanobacterial (CyFBA). In comparison, most of the *N*-(2-benzoylhydrazine-1-carbonothioyl) benzamide derivatives (**L14~L22**) exhibit higher CyFBA-II inhibitory activities compared to *N*-(phenylcarbamothioyl) benzamide derivatives (**L1~L13**). When the OH was introduced on the benzoylhydrazine moiety of the benzamide derivatives, the corresponding compounds, such as **L14**(0.65μM), **L15**(0.63μM) and **L16**(0.88 μM), exhibit high CyFBA-II inhibitory activities. Furthermore, the algicide activities were determined for Synechocystis sp. PCC 6803. The results suggest that most of the compounds with high CyFBA-II inhibition might exhibit potential *in vivo* activities. Especially, compound **L14** not only shows high CyFBA-II activities (K_i = 0.65 μM), but also exhibits highest algicide activities (EC_{50} = 0.09 ppm), which is 7-fold potent than our previous inhibitor (EC_{50}=0.6 ppm). The possible interactions of representative compound **L14** and surrounding key residues in the active site of CyFBA-II were elucidated by jointly using DOX, MD simulations, MM-PBSA and Site-directed mutagenesis assays. The well agreement between theoretical and experimental results suggest that the DOX strategy is a reliable approach for the prediction of the binding-model of inhibitor and target, and the present design strategies were successfully implemented to rapidly screen and optimization of novel inhibitors. The satisfactory algicide activities suggest that the thiourea derivatives are very likely to be a promising lead compound for the development of novel specific algicides to solve CHABs.

4. Experimental

4.1. Molecular dynamics (MD) simulations and Binding Free Energies

To verify the binding mode of hit compounds and CyFBA-II, the MD simulations were further performed by using pmemd.cuda module of AMBER16. The hit compounds were optimized by Gaussian 09 at the ωb97xd/6-31g(d) level, and the whole protein was optimized using Amber force field. The AMBER10 force field and gaff force field were used for CyFBA-II and inhibitors, respectively. The whole system was immersed with TIP3P water molecules[31] in a truncated octahedron box of 10 Å from any solute atoms. The system was neutralized with the counterions of Na^+. SHAKE[32] was used to constrain bonds involving hydrogen atoms, and the time step was 2.0 fs. the long-range electrostatics were calculated by the particle mesh Ewald (PME) algorithm.[33] The nonbonded cutoff was set to 10 Å. Based on the MD trajectories, the binding free energies **L14** were also calculated using MM/GBSA. The electrostatic desolvation free energy was calculated by the Generalized Born (GB) model.[34] The binding interface of CyFBA-II (or it's mutant) and inhibitor is relatively hydrophobic. The solvent and the solute dielectric constants of GB were set to 80 and 1, respectively.[35] The nonpolar desolvation term was estimated from the solvent accessible surface area (SASA): 0.0072 × SASA + 0.00.[36]

4.2. Chemicals and Reagents.

The proton (^{1}H) and carbon (^{13}C) NMR spectra were recorded on a Varian Mercury-Plus 400 or 600 MHz spectrometer in $CDCl_3$, DMSO-d_6 or acetone-d_6. Chemical shifts were given in parts per million (ppm) with TMS as the internal reference. Flash chromatography purifications were performed on Merck silica gel 60 (230−400 mesh) as the stationary phase, and MeOH and CH_3COCH_3 were used as eluents. High-resolution mass spectrometry (HRMS) analysis was performed using a hydride IT-TOF mass spectrometer with ESI interface (Shimadzu, Kyoto, Japan) and Agilent 6224 Accurate-Mass time-of-flight mass spectrometer with ESI interface (Agilent Technologies, Waldbronn, Germany). The synthetic procedure, ^{1}H and ^{13}C nuclear magnetic resonance (NMR) and high-resolution mass specitrometry (HRMS) are listed in the Supporting Information.

4.3. Enzyme inhibition activities and Site-Directed Mutagenesis.

Triosephosphate isomerase (TIM), glycerol 3-phosphate dehydrogenase (GPDH), and FBA-I were from rabbit muscle and purchased from Sigma Corporation. The inhibition constant (K_i) of the hit compounds were determined at the CyFBA-II (or it's mutant) recombinant protein level as described previously.[37] The recombinant protein was expressed in E. coli BL21(DE3) cells, it was purified as previous document.[9, 37] Commercial preparations from Sigma of glycerol 3-phosphate dehydrogenase (GPDH) from rabbit muscle and triosephosphate isomerase (TIM) from rabbit muscle were used. The inhibitory activity of hit compounds against CyFBA-II were determined by using an NADH linked enzymatic assay.[38, 39] The activity of cleavage reaction was examined in Tris-HCl buffer (50mM, pH 7.5), NADH (0.6 mM), glycerol 3-phosphate dehydrogenase (GPDH, 0.3 U, Sigma), triosephosphate isomerase (TIM, 1 U, Sigma), aldolase (1.4 μg/mL), and various concentrations of fructose-1, 6-bisphosphate (FBP, 0.04–5mM) in a cuvette to give the final volume of 0.4 mL. The reaction progress was measured by monitoring the change in absorbance of NADH at 340 nm on the microplate reader (SpectraMax M5, Molecular Devices) over 5 min at 30 °C. The dose-response curves of compounds **L10**, **L11**, **L14**, **L15** and **L16** against wild-type CyFBA-II were illustrated in **Figure S5**.

K_i values were determined by the inhibition of the reaction at more than two concentrations of the substrate (FBP). In present study, The **L11** and **L14** were selected for the validation of the competitive inhibitors, as shown in **Figure S6**. For the competitive inhibitors, K_i may be calculated by the equation[40]: $K_i = IC_{50}/(1+S/K_m)$, where IC_{50} is the half-maximal inhibitory concentration, S is the concentration of FBP and K_m is the Michaelis-Menten constant. The K_m value of CyFBA-II is 68 μM. The inhibition rate (I%) was calculated using the following formula: $I\% = [(V_0-V)/V_0] \times 100\%$, where V_0 represent the maximum velocity ($[I]$ = 0 μM), and V indicate the velocity when an inhibitor was added. All data were analyzed by GraphPad Prism 6.0 software (Prism Software).

Mutations were performed by introducing specific base changes into a double-stranded DNA plastid. All highly effective site-directed mutagenesis were performed using KODPlus Mutagenesis kit (Toyobo, Osaka, Japan) in term of the manufacturer's protocol as our previous document.[41] The wild-type CyFBA-II plasmid and mutagenic primers were denatured, annealed, and polymerized in a final volume of 50 μL for 25 cycles (95 °C for 30s, 60 °C for 1 min, and 72 °C for 3 min). Additionally, *Nde I* and *BamH I* restriction enzyme (Fermentas, China) was used to digest the parental methylated and hemi-methylated DNA. Then, the plasmids of mutations were transformed into *Escherichia coli* (*E. coli*) strain BL21 (DE3) cells, and the sequence analysis were performed for validations. By using SDS-PAGE, the identical motilities were exhibited for all purified enzymes (wild and mutants) to ensure the purities more than 90%.

4.4. Inhibitory Assays on Synechocystis sp. PCC 6803.

Synechocystis sp. PCC 6803 were cultured photoautotrophically in BG11 medium[42] at 28 °C, it is in light for 12 h and in dark for 12 h alternatively, and 50−55% relative humidity for seven days in 96-well

microtiter plates as described previously.[9] This is similar to the antibacterial bioassay.[43] The inhibition rate (*I*%) of test compounds on the cyanobacteria growth was determined according to previous work.[8] The half maximal effective concentration (EC_{50}) values were obtained from the inhibition curves for the inhibition rate against various concentrations of hit compounds. The curves were fitted by nonlinear regression using logistic equation in Origin 7.7 software.

Acknowledgments

This work was supported by the Natural Science Foundation of China (Nos. 21877046, 21873035, 21572077 and 21472061), the Program for the PCSIRT (No. IRT0953), and the self-determined research funds of CCNU from the colleges' basic research and operation of MOE (Nos. CCNU18TS010, CCNU18ZDPY02, CCNU16A02041 and CCNU14A05006), the support from the Program of Introducing Talents of Discipline to Universities of China (111 Program, B17019) is also appreciated.

Supplementary Material

Experimental procedures, analytical data, enzyme assays, and biological evaluation. This material can be found online

References and notes

1. Carmichael WW: Health Effects of Toxin-Producing Cyanobacteria:"The CyanoHABs". *Hum. Ecol. Risk Assess.* 2001, **7**(5):1393-1407.
2. Cheung MY: Toxin-producing cyanobacteria in freshwater: A review of the problems, impact on drinking water safety, and efforts for protecting public health. *J. Microbiol.* 2013, **51**(1):1-10.
3. Chan AN, Shiver AL, Wever WJ, Razvi SZ, Traxler MF, Li B: Role for dithiolopyrrolones in disrupting bacterial metal homeostasis. *Proc. Natl. Acad. Sci. U S A* 2017, **114**(10):2717-2722.
4. Tran H-T, Lee S-H, Ho T-H, Hong S-H, Huynh K-H, Ahn Y-J, Oh D-K, Kang L-W: Crystallographic snapshots of active site metal shift in E. coli fructose 1,6-bisphosphate aldolase. *BMB Reports* 2016, **49**(12):681-686.
5. Obexer R, Godina A, Garrabou X, Mittl PRE, Baker D, Griffiths AD, Hilvert D: Emergence of a catalytic tetrad during evolution of a highly active artificial aldolase. *Nat. Chem.* 2017, **9**(1):50-56.
6. Ziveri J, Tros F, Guerrera IC, Chhuon C, Audry M, Dupuis M, Barel M, Korniotis S, Fillatreau S, Gales L *et al*: The metabolic enzyme fructose-1,6-bisphosphate aldolase acts as a transcriptional regulator in pathogenic Francisella. *Nat. Commun.* 2017, **8**(1):848-853.
7. Ogawa T, Murakami K, Yoshino M: Inhibition by fructose 1,6-bisphosphate of transaldolase from Escherichia coli. *FEMS Microbiol. Lett.* 2016, **363**(17).
8. Han X, Zhu X, Zhu S, Wei L, Hong Z, Guo L, Chen H, Chi B, Liu Y, Feng L *et al*: A Rational Design, Synthesis, Biological Evaluation and Structure–Activity Relationship Study of Novel Inhibitors against Cyanobacterial Fructose-1,6-bisphosphate Aldolase. *J. Chem. Inf. Model.* 2016, **56**(1):73-81.
9. Li D, Han XY, Tu QD, Feng LL, Wu D, Sun Y, Chen HF, Li YJ, Ren YL, Wan J: Structure-Based Design and Synthesis of Novel Dual-Target Inhibitors against Cyanobacterial Fructose-1,6-Bisphosphate Aldolase and Fructose-1,6-Bisphosphatase. *J. Agric. Food Chem.* 2013, **61**(31):7453-7461.
10. Rao L, Chi B, Ren Y, Li Y, Xu X, Wan J: DOX: A new computational protocol for accurate prediction of the protein–ligand binding structures. *J. Comput. Chem.* 2016, **37**(3):336-344.

11. Miller BR, 3rd, McGee TD, Jr., Swails JM, Homeyer N, Gohlke H, Roitberg AE: MMPBSA.py: An Efficient Program for End-State Free Energy Calculations. *J. Chem. Theory Comput.* 2012, **8**(9):3314-3321.
12. Erlanson DA, Fesik SW, Hubbard RE, Jahnke W, Jhoti H: Twenty years on: the impact of fragments on drug discovery. *Nat. Rev. Drug Discov.* 2016, **15**(9):605-619.
13. Fuller N, Spadola L, Cowen S, Patel J, Schonherr H, Cao Q, McKenzie A, Edfeldt F, Rabow A, Goodnow R: An improved model for fragment-based lead generation at AstraZeneca. *Drug Discov. Today* 2016, **21**(8):1272-1283.
14. Böhm H-J: The computer program LUDI: A new method for the de novo design of enzyme inhibitors. *J. Comput. Aided Mol. Des.* 1992, **6**(1):61-78.
15. Liu Q, Masek B, Smith K, Smith J: Tagged fragment method for evolutionary structure-based de novo lead generation and optimization. *J. Med. Chem.* 2007, **50**(22):5392-5402.
16. Gillet VJ, Newell W, Mata P, Myatt G, Sike S, Zsoldos Z, Johnson AP: SPROUT: recent developments in the de novo design of molecules. *J. Chem. Inf. Comput. Sci.* 1994, **34**(1):207-217.
17. Roe DC, Kuntz ID: BUILDER v.2: Improving the chemistry of a de novo design strategy. *J. Comput. Aided Mol. Des.* 1995, **9**(3):269-282.
18. Waszkowycz B, Clark DE, Frenkel D, Li J, Murray CW, Robson B, Westhead DR: PRO_LIGAND: an approach to de novo molecular design. 2. Design of novel molecules from molecular field analysis (MFA) models and pharmacophores. *J. Med. Chem.* 1994, **37**(23):3994-4002.
19. Wang R, Gao Y, Lai L: LigBuilder: A Multi-Purpose Program for Structure-Based Drug Design. *Mol. Model. Annual* 2000, **6**(7-8):498-516.
20. Douguet D, Munierlehmann H, Labesse G, Pochet S: LEA3D: a computer-aided ligand design for structure-based drug design. *J. Med. Chem.* 2005, **48**(7):2457-2468.
21. Svensson F, Bender A, Bailey D: Fragment-Based Drug Discovery of Phosphodiesterase Inhibitors. *J. Med. Chem.* 2018, **61**(4):1415-1424.
22. Hao G-F, Wang F, Li H, Zhu X-L, Yang W-C, Huang L-S, Wu J-W, Berry EA, Yang G-F: Computational Discovery of Picomolar Qo Site Inhibitors of Cytochrome bc1 Complex. *J. Am. Chem. Soc.* 2012, **134**(27):11168-11176.
23. Li Y, Zhao Z, Liu Z, Su M, Wang R: AutoT&T v.2: An Efficient and Versatile Tool for Lead Structure Generation and Optimization. *J. Chem. Inf. Model.* 2016, **56**(2):435-453.
24. Han X, Zhu X, Hong Z, Wei L, Ren Y, Wan F, Zhu S, Peng H, Guo L, Rao L *et al*: Structure-Based Rational Design of Novel Inhibitors Against Fructose-1,6-Bisphosphate Aldolase from Candida albicans. *J. Chem. Inf. Model.* 2017, **57**(6):1426-1438.
25. Jain A: Surflex-Dock 2.1: Robust performance from ligand energetic modeling, ring flexibility, and knowledge-based search. *J. Comput. Aided Mol. Des.* 2007, **21**(5):281-306.
26. Wang J, Hou T: Drug and drug candidate building block analysis. *J. Chem. Inf. Model.* 2010, **50**(1):55-67.
27. Pang YP, Davis J, Wang S, Park JG, Nambiar MP, Schmidt JJ, Millard CB: Small molecules showing significant protection of mice against botulinum neurotoxin serotype A. *PLoS One* 2010, **5**(4):e10129.
28. Pang YP, Vummenthala A, Mishra RK, Park JG, Wang S, Davis J, Millard CB, Schmidt JJ: Potent new small-molecule inhibitor of botulinum neurotoxin serotype A endopeptidase

developed by synthesis-based computer-aided molecular design. *PLoS One* 2009, **4**(11):e7730.

29. Wang R, Yipin Lu A, Wang S: Comparative Evaluation of 11 Scoring Functions for Molecular Docking. *J. Med. Chem.* 2003, **46**(12):2287-2303.
30. Rauf MK, Talib A, Badshah A, Zaib S, Shoaib K, Shahid M, Flörke U, Imtiaz ud D, Iqbal J: Solution-phase microwave assisted parallel synthesis of N,N′-disubstituted thioureas derived from benzoic acid: Biological evaluation and molecular docking studies. *Eur. J. Med. Chem.* 2013, **70**:487-496.
31. Jorgensen WL, Chandrasekhar J, Madura JD, Impey RW, Klein ML: Comparison of simple potential functions for simulating liquid water. *J. Chem. Phys.* 1983, **79**(2):926-935.
32. Ryckaert J-P, Ciccotti G, Berendsen HJC: Numerical integration of the cartesian equations of motion of a system with constraints: molecular dynamics of n-alkanes. *J. Comput. Phys.* 1977, **23**(3):327-341.
33. Darden T, York D, Pedersen L: Particle mesh Ewald: An N·log(N) method for Ewald sums in large systems. *J. Chem. Phys.* 1993, **98**(12):10089-10092.
34. Tsui V, Case DA: Theory and applications of the generalized Born solvation model in macromolecular simulations. *Biopolymers* 2000, **56**(4):275-291.
35. Hou T, Wang J, Li Y, Wang W: Assessing the performance of the molecular mechanics/Poisson Boltzmann surface area and molecular mechanics/generalized Born surface area methods. II. The accuracy of ranking poses generated from docking. *J. Comput. Chem.* 2011, **32**(5):866-877.
36. Weiser Jr, Shenkin PS, Still WC: Approximate atomic surfaces from linear combinations of pairwise overlaps (LCPO). *J. Comput. Chem.* 1999, **20**(2):217-230.
37. Nakahara K: Purification and Characterization of Class-I and Class-II Fructose-1,6-bisphosphate Aldolases from the Cyanobacterium Synechocystis sp. PCC 6803. *Plant Cell Physiol.* 2003, **44**(3):326-333.
38. Racker E: Spectrophotometric measurement of hexokinase and phosphohexokinase activity. *J. Biol. Chem.* 1947, **167**(3):843-854.
39. Blonski C, De Moissac D, Perie J, Sygusch J: Inhibition of rabbit muscle aldolase by phosphorylated aromatic compounds. *Biochem. J.* 1997, **323**:71-77.
40. Yung-Chi C, Prusoff WH: Relationship between the inhibition constant (KI) and the concentration of inhibitor which causes 50 per cent inhibition (I50) of an enzymatic reaction. *Biochem. Pharmacol.* 1973, **22**(23):3099-3108.
41. Li D, Gui J, Li YJ, Feng LL, Han XY, Sun Y, Sun TL, Chen ZG, Cao Y, Zhang Y *et al*: Structure-Based Design and Screen of Novel Inhibitors for Class II 3-Hydroxy-3-methylglutaryl Coenzyme A Reductase from *Streptococcus Pneumoniae*. *J. Chem. Inf. Model.* 2012, **52**(7):1833-1841.
42. R Y Stanier RK, M Mandel, and G Cohen-Bazire: Purification and Properties of Unicellular Blue-Green Algae (Order hroococcales). *Bacteriol. Rev.* 1971, **35(2)**:171-205.
43. Xiao J, Zhang Q, Gao YQ, Tang JJ, Zhang AL, Gao JM: Secondary metabolites from the endophytic Botryosphaeria dothidea of Melia azedarach and their antifungal, antibacterial, antioxidant, and cytotoxic activities. *J. Agric. Food Chem.* 2014, **62**(16):3584-3590.

Graphical Abstract

To create your abstract, type over the instructions in the template box below.
Fonts or abstract dimensions should not be changed or altered.

Design, synthesis and algicides activities of thiourea derivatives as the Novel Scaffold Aldolase Inhibitors

Leave this area blank for abstract info.

Shan Xiao, Lin Wei, Zongqin Hong, Yanliang Ren*, Li Rao, Lingling Feng and Jian Wan*

International Cooperation Base of Pesticide and Green Synthesis (Hubei), Key Laboratory of Pesticide & Chemical Biology (CCNU), Ministry of Education, Department of Chemistry, Central China Normal University, Wuhan 430079, China